CHAPTER 5

Sintering and Corrosion Resistance

THE PRIMARY GOAL in stainless steel sintering is to obtain good corrosion resistance along with good mechanical properties and adequate dimensional tolerances. Most aspects of sintering have a bearing on corrosion resistance; therefore, in the following, sintering is discussed with an emphasis on its effect on corrosion resistance.

In wrought stainless steels, superior corrosion resistance is of paramount importance, because mechanical properties similar to and even superior to stainless steels can be obtained much less expensively with conventional carbon steels. However, over several decades, despite modest corrosion resistances, commercial sintered stainless steels found niche applications (for example, office machine parts, lock parts, mirror mounts, some appliance parts, etc.) where sintered stainless steels were able to compete with wrought or cast stainless steels because their corrosion properties met the moderate requirements. Also, powder metallurgy (PM) parts offered their typical advantages: good material utilization and low-cost net shape fabrication (no machining costs).

From the 1950s until the mid-1980s, belt furnaces were the dominant method of industrial sintering of stainless steels in North America. Maximum sintering temperature was approximately 1150 °C (2100 °F), and furnace atmosphere was dissociated ammonia (DA). The lower-cost atmosphere and the higher strength levels possible with sintering in DA were attractive, but it was also more difficult to achieve good corrosion properties in DA than in hydrogen or vacuum. Hence, the gradual shift to hydrogen and vacuum sintering, or the use of a $90H_2$-$10N_2$ atmosphere, during the past 10 years. There was also a shift toward high-temperature (>1205 °C, or >2200 °F) sintering.

The majority of studies on the corrosion resistance of sintered stainless steels still lack a full description of the experimental conditions employed. The most frequently omitted process parameters are the dewpoint of the sintering atmosphere and the cooling rate after sintering. Because these and other parameters are of critical importance to corrosion properties of sintered stainless steels, only publications providing critical processing data and/or permitting unambiguous conclusions are reviewed in the context of corrosion-resistance properties.

If sintering conditions are conducive to the development of good corrosion resistance, good mechanical properties usually follow. The reverse is not necessarily true. Each sintering atmosphere has its own peculiarities with regard to stainless steels, mainly because each responds differently to a number of chemical reactions involving the interstitials carbon, nitrogen, and oxygen. The details of these reactions largely determine the corrosion and dynamic mechanical properties of sintered parts. The many misconceptions about sintering stainless steels (Table 1.1 in Chapter 1, "Introduction") arise in large part from a lack of appreciation of the importance of these chemical reactions and from ignoring their differences for the various sintering atmospheres. Even though the extent of these reactions typically varies from only several hundred to a few thousand parts per million, they are of critical importance. Viewing the sintering atmosphere as mainly an inert cover to protect parts from oxidation, typical of the early years, grossly misjudges its importance.

In wrought stainless steel technology, oxygen, carbon, and nitrogen are controlled at the refining stage of the production process; in PM, they are controlled during powder manufacture and sintering. Excessive amounts of carbon and nitrogen can give rise to the formation of chromium carbides and chromium nitride, with negative effects on corrosion resistance. These

precipitates can be identified metallographically and through special corrosion tests. Furthermore, they resemble the corresponding phenomena in wrought stainless steels. However, precipitates of silicon dioxide that form during cooling after sintering usually do not show up in a metallographic cross section and are normally absent in properly finished wrought stainless steels.

5.1 Sintering Furnaces and Atmospheres

Notwithstanding the importance of powder selection, the sintering process is of even greater importance for the successful processing of stainless steels. It encompasses many more elements, from furnace type and atmosphere choice to process parameter choices. All of these influence the quality of a sintered part. To the extent that these elements are common to general PM processing, their treatment in the following is only cursory. For a detailed general treatment of both practice and fundamentals of sintering, the reader is advised to consult the literature sources suggested at the beginning of Chapter 1, "Introduction." However, those elements and parameters that have a special bearing on sintered stainless steels, both regarding their mechanical properties and, more so, their corrosion-resistance properties, are treated in detail.

Sintering Furnaces. Most commercial sintering of stainless steel parts is performed in continuous mesh belt conveyor furnaces at temperatures up to approximately 1150 °C (2100 °F). Pusher, walking beam, and vacuum furnaces are used for higher temperatures up to approximately 1345 °C (2450 °F). In recent years, ceramic belt furnaces have also been introduced for high-temperature sintering. The higher temperatures are favored for improved mechanical and corrosion properties. Vacuum and other high-temperature furnaces began to be more widely used in the 1980s, as a result of increasing demands on magnetic and corrosion-resistance properties. Although some sintering furnaces for carbon steel parts now have gas quench capability in their cooling zones, permitting so-called sinter hardening, most industrial furnaces for stainless steels presently lack this feature, despite its benefits in minimizing reoxidation in the cooling zone and reducing the risk of sensitization. In this regard, vacuum furnaces, with their readily available gas quench features, are advantageous. Among the belt furnace types, so-called humpback furnaces (Fig. 5.1) (Ref 1), give lower dewpoints. Their inclined entrance and exit zones retain the lighter hydrogen better than the more common horizontal furnaces.

It is the inferior control of dewpoint and slower cooling after sintering in many commercial furnaces, compared to laboratory furnaces, that has led to one of the half-truths (Table 1.1 in Chapter 1) about the corrosion resistance of stainless steel parts, namely, that PM parts possessing good corrosion resistance can be produced in laboratory furnaces but not in industrial furnaces.

Sintering Atmospheres. Typical sintering atmospheres for stainless steels include hydrogen, hydrogen-nitrogen mixtures, dissociated ammonia, and vacuum. Because a low-dewpoint capability is important for both hydrogen and hydrogen-nitrogen atmospheres, there is a widespread belief throughout the industry that the use of cryogenic nitrogen in hydrogen-nitrogen mixtures makes it easier to attain the required low dewpoints because of the dryness of cryogenic nitrogen. However, the reducibility criterion for nitrogen-containing hydrogen demands lower dewpoints than those for pure hydrogen (Fig. 5.15).

Dissociated ammonia with dewpoints of approximately –45 °C (–50 °F) was the most

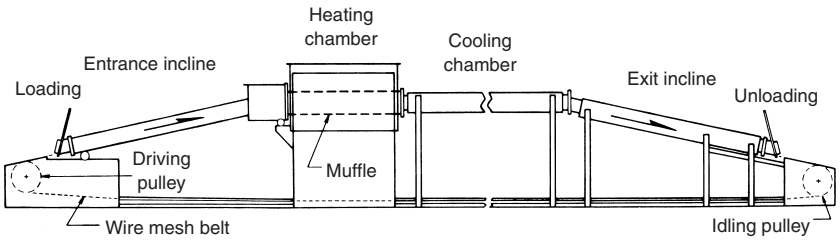

Fig. 5.1 Schematic of a humpback mesh belt furnace. Source: Ref 1. Reprinted with permission from MPIF, Metal Powder Industries Federation, Princeton, NJ

widely used sintering atmosphere until the mid-1980s. In the interest of high-strength parts and low-cost sintering atmospheres, some stainless steel parts were even sintered in N_2-H_2 atmospheres containing as little as 3% H_2. As is shown later, such parts had very low corrosion-resistance requirements. Vacuum sintering of stainless steels is conducted with low pressures (1000 to 3000 μm Hg) of argon or nitrogen to minimize chromium losses due to the high vapor pressure of that element at elevated temperature (section 5.2.5 in this chapter).

5.2 Sintering of Stainless Steels

Prior to actual sintering, PM parts are delubricated either as part of the sintering process or in a separate step. The importance of delubrication for stainless steels had been underrated for many years, with the result that parts possessed excessive carbon contents due to lubricant decomposition. If the furnace temperature rises above approximately 540 to 650 °C (1000 to 1200 °F) before most of the lubricant has had time to volatilize, lubricant decomposition and carbon absorption by the part will take place rather than lubricant volatilization. While vacuum furnaces can readily cope with carbon absorption (section 5.2.5 in this chapter), lowering carbon levels in hydrogen and hydrogen-nitrogen atmospheres is more difficult. This subject is discussed in section 5.2.3 in this chapter.

5.2.1 Fundamental Relationships

The development of properties of stainless steels as a function of density and sintering temperature is similar to those of carbon steels. Figures 5.2 (Ref 2) and 5.3 (Ref 3) illustrate some of the basic relationships between sintering temperature, sintered density, and properties of parts. Corresponding explicit data for sintered stainless steels are given in Chapter 7, "Mechanical Properties."

In addition to the effect of density, sintered steels differ from similar wrought steels in that they usually possess smaller grain size. High-temperature-sintered ferritic stainless steels, however, possess large grain sizes. Also, inclusions and second phases are distributed throughout the matrix rather uniformly, and the oxygen contents are often an order of magnitude higher than those in wrought stainless steels. The latter arises from the oxidation during water atomization of a stainless steel powder (section 3.1.5 in Chapter 3, "Manufacture and Characteristics of Stainless Steel Powders"). Typical commercial sintering conditions remove or reduce only a small portion of this oxygen.

In order for mechanical properties to develop properly and in a reasonable amount of time, it is critical that atomic diffusion during sintering is not impeded by the oxide layers of the water-atomized powder particles. In the case of plain iron powders, such oxides are readily reduced by any of the common sintering atmospheres. In the case of water-atomized stainless steels, much drier (lower-dewpoint) atmospheres are necessary for reduction. Residual oxides, sometimes termed acid insolubles, can reduce the mechanical properties of a sintered part. Dautzenberg and Gesell (Ref 4) showed that the ultimate tensile strength of a sintered austenitic stainless steel was increased by 30% when its oxygen content was decreased from 1.0 to 0.2%. Although

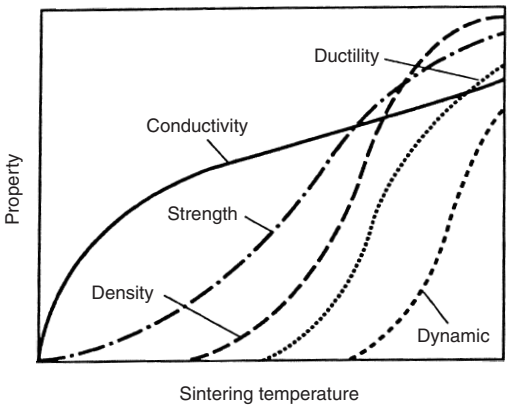

Fig. 5.2 Variation in compact properties with degree of sintering, as represented by sintering temperature. Source: Ref 2. Reprinted with permission from MPIF, Metal Powder Industries Federation, Princeton, NJ

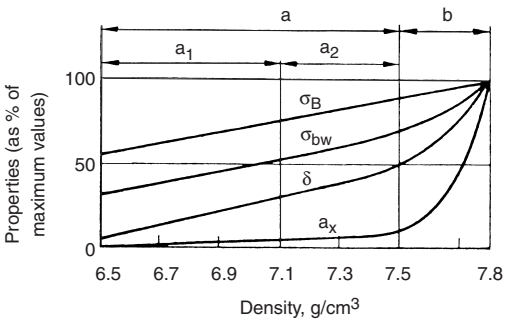

Fig. 5.3 Correlation of process-dependent density and important properties. Source: Ref 3

acceptable mechanical properties (acceptable in this case means that sintered parts will meet the properties specified in Metal Powder Industries Federation, or MPIF, and ASTM standards) are obtainable with the common industrial sintering atmospheres and with sintering times of only 30 min, sintering under conditions that lower the amount of oxygen (oxides) clearly and significantly improves the dynamic mechanical properties of sintered stainless steels, that is, fatigue and impact strength.

For the same fundamental reason, properties of fully dense parts, made from gas-atomized powders with low oxygen contents and/or low contents of undesirable interstitials, can be superior to their wrought counterparts because of their lower levels of interstitials and the more uniform (isotropic) distribution of these interstitials within the matrix. Superior mechanical and corrosion-resistance properties have been documented for fully dense PM stainless steels, PM superalloys, and PM aluminum alloys (Ref 5).

For vacuum sintering at high temperature (>1200 °C, or >2192 °F), the addition of graphite to the stainless steel powder prior to compacting can produce oxygen contents of less than 300 ppm, with carbon contents of less than 0.03% (section 5.2.5 in this chapter) and a 40% improvement in impact strength (Ref 6).

In hydrogen-nitrogen atmospheres, lower dewpoint and higher hydrogen content give better reduction of oxides. Lower compact density will also produce lower oxygen contents because of faster diffusion of the reducing gas and reaction products (H_2O, CO, CO_2). Longer sintering time, of course, will also result in more reduction.

Differences in the mechanical properties of sintered stainless steels as well as in their dimensional change (whether from lot to lot or from producer to producer) are mainly caused by differences in the amount and distributions of the interstitials, oxygen, carbon, and nitrogen. These in turn arise from differences in processing. With good sintering practice, homogenization of the microstructure takes place quite rapidly. This is described in more detail in section 5.2.3 in this chapter.

While it is possible to obtain good corrosion resistance in any of the common sintering atmospheres, each atmosphere demands its own controls. It is therefore convenient to discuss this subject individually for each sintering atmosphere. However, the control of sintered density and how it affects corrosion resistance is common to all types of sintering and is therefore addressed now.

5.2.2 *Effect of Sintered Density on Corrosion Resistance*

The corrosion resistance of stainless steels can differ widely, depending on the testing environment. Different mechanisms of corrosion have been correlated with certain environments.

Acidic Environment. Testing of sintered stainless steels in acids, that is, H_2SO_4, HCl, and HNO_3, shows that corrosion resistance, measured as weight loss, improves significantly with increasing density (Fig. 5.4) (Ref 7). This relationship is confirmed elsewhere (Ref 8–10).

The detrimental effect of pores is attributed to two factors: first, to the large internal surface areas of sintered parts, which, at the typical densities of many structural parts (i.e., 80 to 85% of theoretical), are still 2 orders of magnitude larger than their exterior geometric surface areas and therefore can be subject to increased general corrosion; second, to a lack of passivation within the pores of a sintered part. Open-circuit measurements (section 9.1.3 in Chapter 9, "Corrosion Testing and Performance") of wrought stainless steels in an acidic environment show that the potential typically increases with time (Ref 11). This can be interpreted as passivation and/or healing of active areas. In contrast, sintered stainless steels often exhibit decreasing potential, indicating activation of the surface. Itzhak and Aghion (Ref 12) and Raghu et al. (Ref 11) interpret the declining open-circuit potential of sintered stainless steels as gradually increasing

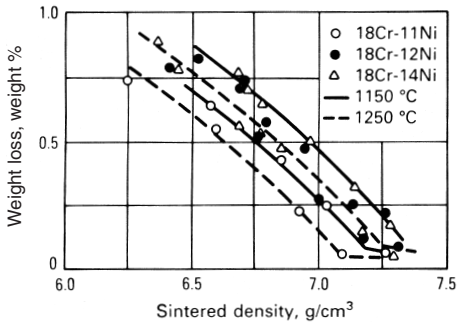

Fig. 5.4 Relationship between sintered density and weight decrease of three austenitic stainless steels in 40% HNO_3. Source: Ref 7. Reprinted with permission from MPIF, Metal Powder Industries Federation, Princeton, NJ

activation as the acid penetrates the pores. This is accompanied by hydrogen evolution on the surface of a part. The main reaction taking place is $2H^+ + 2e^- \rightarrow H_2$. Thus, corrosion in an acidic environment can be viewed as the operation of a hydrogen concentration cell between the external surface of a part and its internal pore surface. The surface of the pores acts as the anode and the engineering surface as the cathode. Metal dissolution occurs primarily in the interior of the material. After 40 h, the activation process comes to an end and the potential increases.

Neutral Chloride-Containing Environment. Corrosion resistance in neutral saline solutions has been found to decline with increasing density (Fig. 5.5) (Ref 13).

The parts of Fig. 5.5 had been prepared from typical –100 mesh compacting-grade powders. The decline of corrosion resistance is moderate at low density but becomes very steep at a relative density of approximately 80 to 84% of theoretical, depending on pore size, pore morphology, and possibly on residual oxygen content. The fact that some specimens in Fig. 5.5 are capable of bridging the low corrosion-resistance gap suggests that the effect is a borderline one and that it may disappear by increasing the intrinsic crevice and pitting resistance of an alloy. In fact, some of the specimens of Fig. 5.5, as a result of carbon-assisted vacuum sintering (section 5.2.5 in this chapter), had very low oxygen contents, comparable to wrought stainless steels. Also, corrosion-resistance/density curves for 317L, a somewhat more corrosion-resistant material because of higher chromium and molybdenum contents, appear to possess a greater number of specimens bridging the corrosion-resistance gap.

Potential-time curves of sintered stainless steels in a neutral saline solution exhibit similar behavior to those in an acidic environment; that is, they also may be characterized by the potential decreasing with time, indicating activation rather than passivation.

Raghu et al. (Ref 14) have performed cyclic potentiodynamic polarization studies on sintered 316L prepared from narrow sieve fractions. Densities varied from 37 to 71%, and testing was performed in 3% NaCl. The difference potential, ΔE, which is a measure for a material susceptibility to crevice corrosion, increased with decreasing pore size (Fig. 5.6)

The detrimental effect of pores is very strong for small pores up to approximately 20 μm (as determined by the bubble point test method for filters) and thereafter becomes much less pronounced. The important variable in this case is pore size rather than porosity.

These results are best explained by assuming the operation of an oxygen concentration cell, which establishes itself in accordance with the mechanism shown in Fig. 5.7 (Ref 15) and Fig. 5.8 (Ref 16).

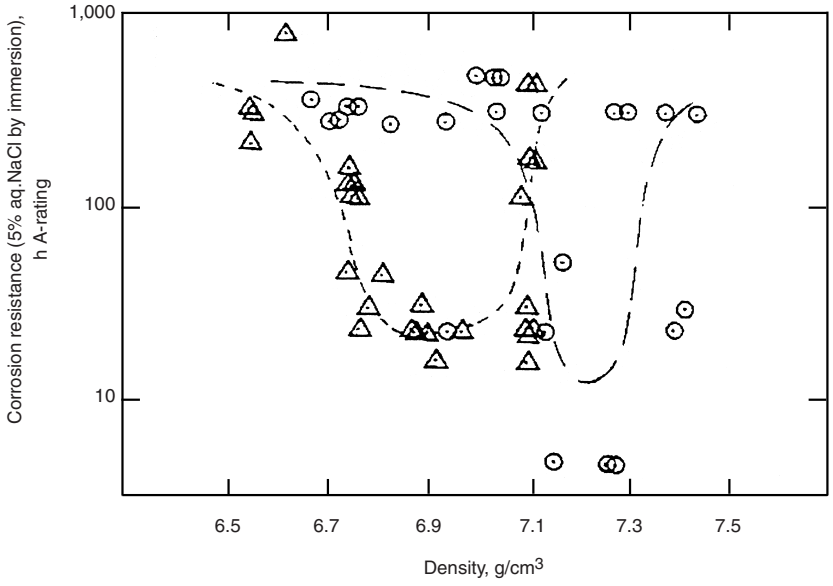

Fig. 5.5 Effect of density on corrosion resistance of 316L parts. Δ, pressed and sintered only; o, pressed, sintered, re-pressed, and annealed. Source: Ref 13. Reprinted with permission from MPIF, Metal Powder Industries Federation, Princeton, NJ

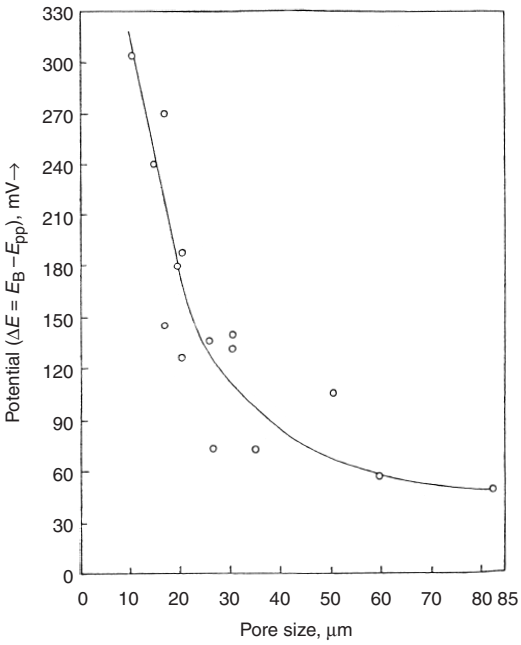

Fig. 5.6 Effect of pore size on size of hysteresis(***E***) for sintered 316L in 3% NaCl (27 °C, or 81 °F). Source: Ref 14. © NACE International 1989

The overall reaction involves the dissolution of metal, M (immersed in aerated saline solution), and the reduction of oxygen to hydroxide in accordance with:

Oxidation

$$M \Rightarrow M^+ + e$$

Reduction

$$O_2 + 2H_2O + 4e \Rightarrow 4OH^-$$

As a result of limited diffusion within the pore space of a part, oxygen within that space becomes depleted and oxygen reduction ceases. However, as shown in Fig. 5.7, metal dissolution continues within the pore space. The latter creates a positive charge (M^+) within the pore space, which is neutralized by the migration of chloride ions into the pore space. The increased metal chloride concentration within the pore space undergoes hydrolyzation into insoluble hydroxide and free acid according to:

$$M^+Cl^- + H_2O = MOH \Downarrow + H^+Cl^-$$

The free acid increases metal dissolution, which in turn increases migration, representing an accelerating, autocatalytic process. As the corrosion within the pore space increases, the

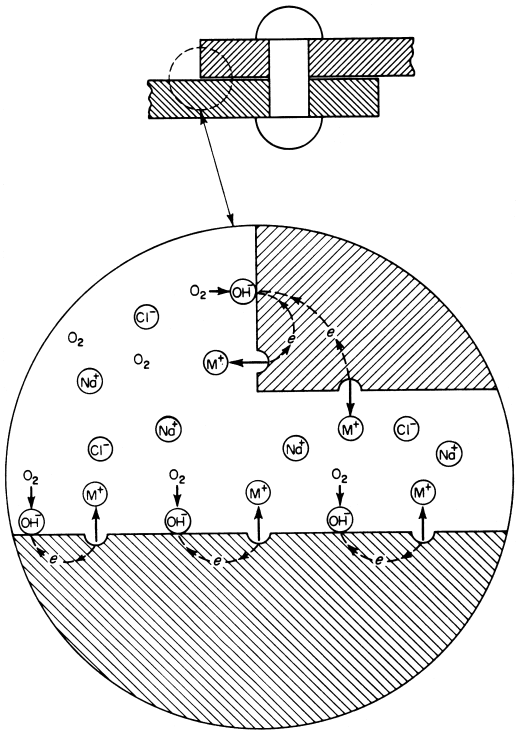

Fig. 5.7 Crevice corrosion mechanism—initial stage. Source: Ref 15. Reprinted with permission, Fontana, *Corrosion Engineering*, 2d ed. © The McGraw-Hill Companies, Inc., 1978

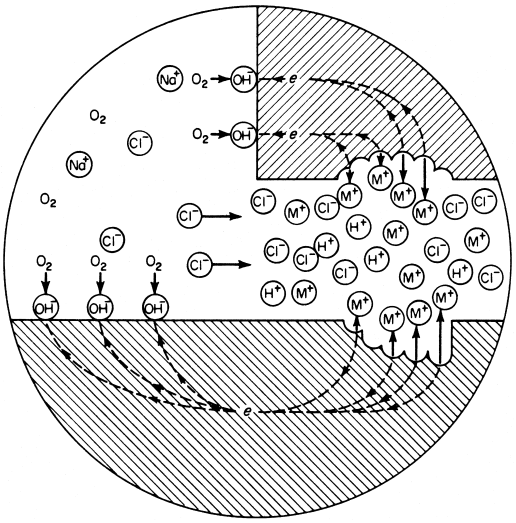

Fig. 5.8 Crevice corrosion mechanism—later stage. Source: Ref 16. Reprinted with permission from MPIF, Metal Powder Industries Federation, Princeton, NJ

rate of oxygen reduction on the internal pore surfaces also increases. This cathodically protects the external surfaces, which explains why during crevice corrosion the attack is localized within the porous or shielded areas, while the remainder suffers little or no damage.

Pore morphology of a sintered part is affected by powder particle shape, particle size distribution, compacting pressure, amount of shrinkage during sintering, re-pressing, and so on. For a stainless steel part made from a typical –100 mesh compacting-grade stainless steel powder, minimum corrosion resistance, as measured by immersion in 5% NaCl, appears at a relative density of approximately 87 to 90%, again depending on pore morphology. Past the minimum, corrosion resistance increases again. The increase past the minimum is attributed to the disappearance of pores as sintered structural parts approach the region of closed-off porosity at approximately 92% of theoretical density. A more uniform density distribution in a sintered part, such as is obtainable with isostatic pressing, or, more practical, with warm compaction, may reduce the width of the crevice-corrosion density regime.

It should be emphasized that corrosion resistance as shown in Fig. 5.5 was measured by the time it took for the development of rust, based on visual assessment. Weight change measurements are not reliable for assessing corrosion resistance of sintered parts that were tested in a neutral environment.

It is not clear why the corrosion resistance at the higher densities past the corrosion-resistance minimum does not approach that of its wrought counterpart. Both pore morphology and residual oxygen content may play a role. In fact, as is shown in section 5.3 on liquid-phase sintering of stainless steels, a high-density, boron-containing, liquid-phase-sintered 316L had a chloride (immersion in 5% aqueous NaCl) corrosion resistance similar to wrought 316L, while other high-density-sintered stainless steels of the same composition but without boron had much lower corrosion resistances. The boron may have scavenged and redistributed the residual oxygen of the sintered material, with the formation of less detrimental borosilicates.

Conflicting with the aforementioned results, short-term potentiodynamic polarization tests by Lei et al. (Ref 17) pointed to a beneficial effect of density in a saline environment. The controversy was resolved when Maahn and Mathiesen (Ref 18) observed that in short-term polarization tests, there was not enough time for the time-consuming buildup of localized attack within pores (Table 5.1) (Ref 19).

While the corrosion resistance related to the outer surfaces, given by i_{peak} and i_{pass}, in general improves with increasing density, with E_{pit} remaining unchanged, more relevant long-term exposure techniques, such as E_{stp} and salt spray testing (NSS1 and NSS2) (Chapter 9, "Corrosion Testing and Performance"), show increasing susceptibility to crevice corrosion with increasing density and increasing oxygen content. Thus, by using slow, stepwise polarization (section 9.1.3 in Chapter 9), the expected relationship—a decrease of the stepwise initiation potential, equivalent to deteriorating corrosion resistance—was observed.

In the past, many instances of corrosion of sintered stainless steels were interpreted as crevice corrosion because of porosity, when in fact they were clearly the result of incorrect or suboptimal sintering that produced metallurgical defects that gave rise to intergranular or galvanic corrosion or that, because of an excessive vacuum (section 5.2.5 in this chapter), led to severe chromium depletion of the surfaces of

Table 5.1 Effect of density and oxygen content on corrosion resistance of hydrogen-sintered 316L

Specimens sintered at 1250 °C (2282 °F), 120 min in pure hydrogen

Compaction pressure		Sintered density,	Open		I_{peak}(a),	I_{pass} (a),	E_{pit} (a),	E_{stp} (b),		
MPa	ksi	g/cm^3	pores, %	O, ppm	μA/cm^2	μA/cm^2	mV SCE	mV SCE	NSS1, h	NSS2
295	43	6.34	19.4	340	31	20	475	0	>1500	9
390	57	6.62	15.5	1260	18	19	425	–100	985	7
490	71	6.86	12.3	970	25	15	475	–75	36	4
540	78	6.94	10.8	1900	18	15	500	–200	60	3
590	86	7.02	9.7	1410	21	14	450	–125	28	2
685	99	7.13	7.6	2150	9	7	500	–225	48	2
785	114	7.23	5.7	2040	7	7	475	–200	24	2

(a) 0.1%Cl$^-$, pH 5, 30 °C (86 °F), 5 mV/min. (b) 5% NaCl$^-$, 30 °C (86 °F), 25 mV/8 h

sintered parts. Mathiesen and Maahn (Ref 20) have used image analysis on 316L parts, sintered in hydrogen under various conditions of time and temperature, to obtain a wide range of sintered densities. Considering the pores as cylindrical holes, they expressed the severity of corrosion in pores as:

$$S = i_a \bullet 1/d$$

where d is the pore diameter, and i_a is the corrosion rate in the passive state. Figure 5.9 shows a plot of the visual rating of corrosion (10 = no rust; 1 = 50% rust) after a 1500 h salt spray test versus the aforementioned severity value.

In the same investigation, Mathiesen and Maahn show that stepwise pitting potential (0.5% Cl) decreases with increasing sintered density of 316L (Table 5.2).

The numbers within the body of Fig. 5.9 refer to the tables of the paper in which the various experiments are described. It is apparent that corrosion resistance begins to deteriorate rapidly at a density of approximately 6.6 g/cm^3 (82% of theoretical). The authors attribute the deterioration of corrosion resistance with increasing density to both a critical pore geometry and to impeded reduction of oxides.

Figure. 5.10 (Ref 15) shows the results of a crevice-corrosion test in accordance with ASTM G 48 wrought 316L and sintered 316L. The density of the sintered 316L was 6.8 g/cm^3 (85% of theoretical), that is, well within the steep decay region for a compacting-grade material.

Interestingly, the sintered part showed only a mild attack in comparison to the severely corroded wrought stainless steel of the same

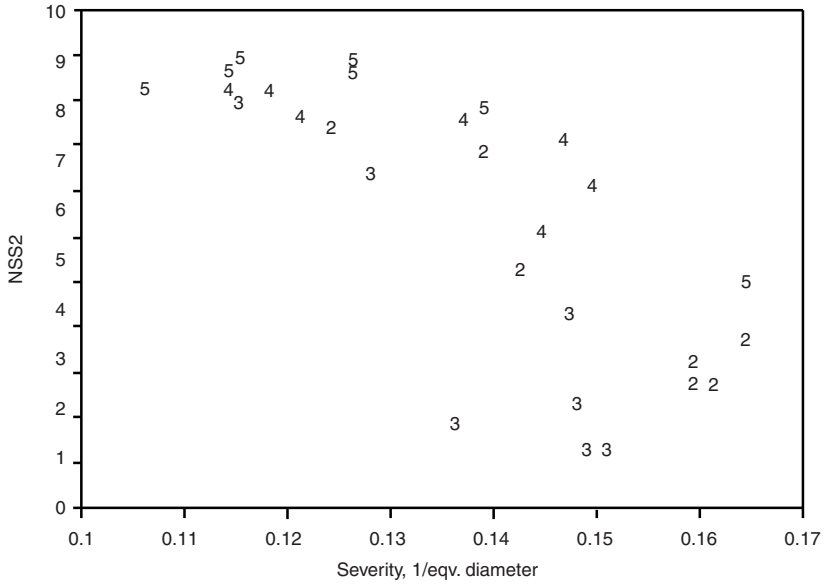

Fig. 5.9 Visual rating after 1500 h salt spray test versus severity value calculated as the reciprocal of average pore diameter. Reprinted with permission from MPIF, Metal Powder Industries Federation, Princeton, NJ

Table 5.2 Effect of density for 316L cylindrical specimens sintered at 1250 °C (2282 °F), 120 min in pure hydrogen

Green density, g/cm^3	Density(a), g/cm^3	Open pores(a),%	Average pore diameter(b), µm	Roundness(b)	NSS1, h	NSS2	Ferroxyl test, Cl^-: 0.5%	E_{stp}(c) mV SCE, Cl^-: 0.1%	E_{stp}(c) mV SCE, Cl^-: 0.5%
5.80	6.40	19.3	9.5	0.73	1336	9	0	350	150
5.91	6.51	17.8	8.8	0.74	>1500	10	0	250	150
6.05	6.65	15.9	8.0	0.72	>1500	10	0	275	100
6.19	6.75	14.4	8.7	0.79	>1500	10	0	250	125
6.25	6.83	13.4	8.0	0.74	>1500	10	0	300	100
6.38	6.93	11.8	7.3	0.75	1168	9	0	325	100
6.44	7.01	10.7	6.1	0.71	192	5	0	300	50

(a) Measured by oil impregnation technique. (b) Measured by image analysis. (c) Stepwise polarization

designation. Evidently, because the entire PM part, on account of its porosity at a relative density of 85%, already represents a system of interconnected crevices, any additional crevice in accordance with ASTM G 48 test seems to have only a minor effect. This relationship is analogous to the lower notch sensitivity of sintered parts in comparison to wrought parts. The authors also found sintered type 304L and 316L stainless steels to be less susceptible to crevice corrosion than wrought 316L, on the basis of the areas of the hysteresis loops of their cyclic polarization curves (Ref 15).

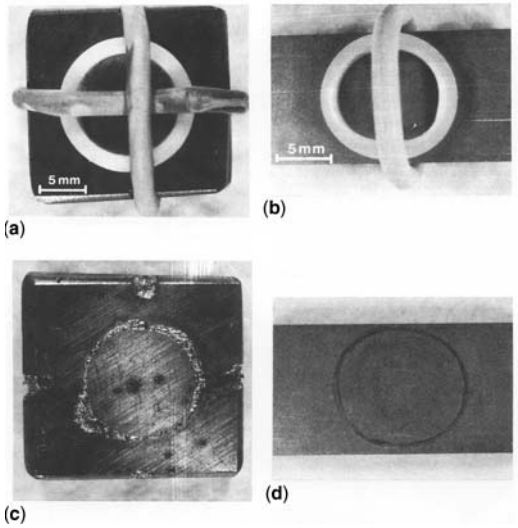

Fig. 5.10 Comparison of wrought and sintered type 316L stainless steels before and after testing in 10% aqueous $FeCl_3$. (a) Assembled crevice-corrosion test specimen of wrought type 316L (100% dense). (b) Assembled crevice-corrosion test specimen of sintered type 316L (85% dense). (c) Wrought specimen after test showing severe attack at four crevices under rubber bands and synthetic fluorine-containing resin ring. (d) Sintered specimen after test showing slight attack under synthetic fluorine-containing resin ring. Source: Ref 15. Reprinted with permission from MPIF, Metal Powder Industries Federation, Princeton, NJ

The reduced crevice sensitivity of sintered stainless steels may be attributed to their interconnected pores, which facilitate oxygen diffusion through and from neighboring pores. As such, it appears that the pore space surrounding a crevice should be taken into account in assessing its susceptibility to crevice corrosion. Oxygen diffusivity within the pore space of a sintered part, as a measure for its capability to transport oxygen to its internal surfaces in order to maintain passivity, appears to be a better characterization for its resistance to crevice corrosion than an average pore diameter. A permeability or diffusivity number takes into account the entire pore space, including its tortuosity. Characterization of the pore space, through mercury porosimetry would also appear to provide more relevant characterization than an average pore diameter. In mercury porosimetry (Fig. 5.11) (Ref 21), the measured pore sizes represent the bottlenecks between neighboring pores rather than pore diameters themselves. It is the totality of these bottlenecks, rather than

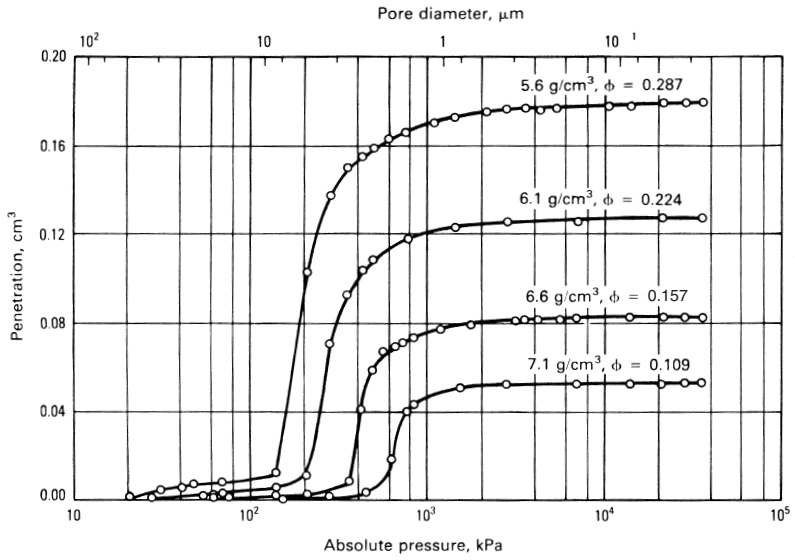

Fig. 5.11 Mercury porosimetry curves of sintered steel parts of varying densities. Green skeletons were sintered at 1093 °C (2000 °F) for 20 min. Total porosity (ϕ) is determined from sample weight and dimensions. Source: Ref 21

the actual pore diameters or pore volumes, that exert the greater influence on a part's capability to facilitate gas diffusion through the pore space. According to Fig. 5.12, the majority of the pore bottlenecks of a sintered steel part (made from a compacting-grade, –100 mesh, water-atomized powder), of a relative density of 80 to 84%, are 4 to 5 μm in size, and at a relative density of 87 to 90%, approximately 2 μm. Assigning greater importance to the bottlenecks would also explain the shift of the crevice-corrosion minimum to a higher density as a result of repressing (Fig. 5.6). In pressing or repressing, densification comes about first through the collapse of the larger pores (Ref 22), whereas in sintering, it is the small pores and the connections between large pores, that is, the aforementioned bottlenecks, that, because of their small curvatures and greater surface energies, become active. Thus, repressing simply increases the density of a part without greatly affecting its bottleneck pores or its diffusivity characteristics, and hence, the shift of maximum corrosion to a higher density.

According to Maahn et al. (Ref 19), the corrosion attack in a ferric chloride test (ASTM G 48) may develop within the pores beneath the surface of a part. In this case, the superior surface appearance of a sintered part may be misleading, and interior examination and testing for mechanical property degradation is appropriate.

For a better assessment of the effect of pore morphology on crevice-corrosion resistance in the low-density range below approximately 80% of theoretical, optimally sintered parts with oxygen contents below approximately 200 ppm should be evaluated. Such parts could be prepared with carbon-assisted optimal vacuum sintering, or, easier, by optimal gravity sintering of a low-oxygen-content, inert-gas-atomized stainless steel powder, or by warm compaction and sintering of such a powder.

Molins et al. (Ref 23) have investigated the influence of several finishing operations on the corrosion resistance of sintered 316L as measured potentiodynamically according to ASTM B 627 in a solution of 0.1 *N* NaCl and 0.4 *N* $NaClO_4$ (Fig. 5.12).

Worsening passivation due to tumbling was interpreted as due to smearing of pores and potential contamination from additives. The best and most significant improvement resulted from operations that sealed surface porosity: grinding, turning, and shot blasting.

It should be stressed again that the effectiveness and/or ranking of such treatments will depend on the quality of sintering. Thus, while any such results may be relevant and practical

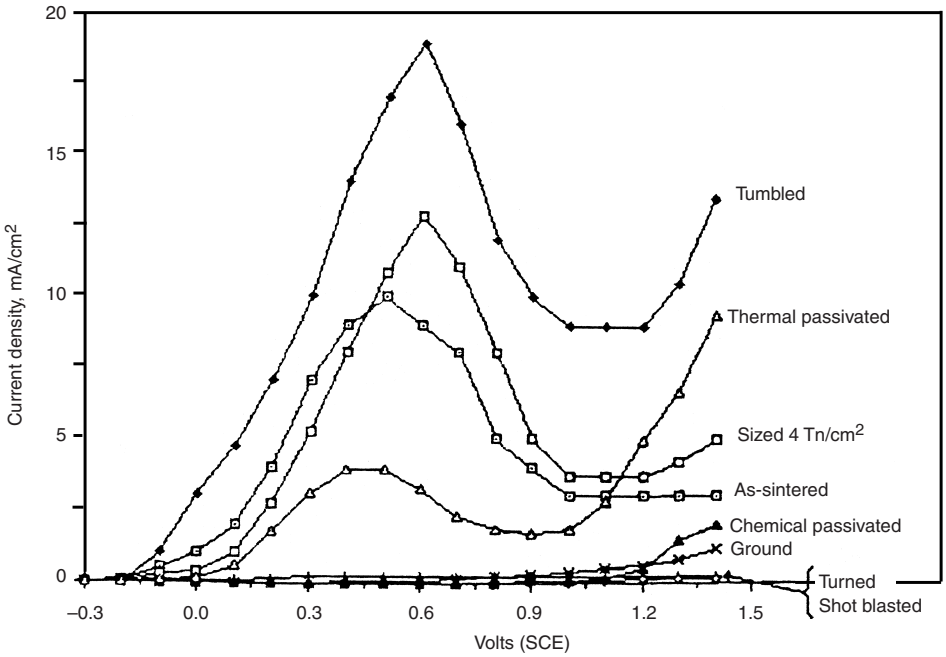

Fig. 5.12 Potentiodynamic curves of 316L stainless steels as a function of surface finishing treatment. Reprinted with permission from MPIF, Metal Powder Industries Federation, Princeton, NJ